Resonant Emittance Mixing of Flat Beams in Plasma Accelerators

S. Diederichs,[1,2] C. Benedetti,[3] A. Ferran Pousa,[1] A. Sinn,[1] J. Osterhoff,[1,3] C. B. Schroeder,[3,4] and M. Thévenet[1,*]
[1]Deutsches Elektronen-Synchrotron DESY, Notkestrasse 85, 22607 Hamburg, Germany
[2]CERN, Esplanade des Particules 1, 1211 Geneva, Switzerland
[3]Lawrence Berkeley National Laboratory, 1 Cyclotron Road, Berkeley, California 94720, USA
[4]Department of Nuclear Engineering, University of California, Berkeley, California 94720, USA

(Received 8 March 2024; revised 30 August 2024; accepted 22 November 2024; published 31 December 2024)

Linear colliders rely on high-quality flat beams to achieve the desired event rate while avoiding potentially deleterious beamstrahlung effects. Here, we show that flat beams in plasma accelerators can be subject to quality degradation due to emittance mixing. This effect occurs when the beam particles' betatron oscillations in a nonlinearly coupled wakefield become resonant in the horizontal and vertical planes. Emittance mixing can lead to a substantial decrease of the luminosity, the main quantity determining the event rate. In some cases, the use of laser drivers or flat particle beam drivers may decrease the fraction of resonant particles and, hence, mitigate emittance deterioration.

DOI: 10.1103/PhysRevLett.133.265003

Plasma-based accelerators [1,2] are promising candidates as drivers for future linear colliders due to their $\gtrsim$ GV/m accelerating gradients. Although experimental progress in terms of energy gain [3–5], energy transfer efficiency [6], and energy spread preservation [7,8] have increased the interest in plasma-based linear colliders [9–11], additional challenges must be overcome.

For optimal operation of a linear collider, the event rate and, consequently, the luminosity $\mathcal{L}$ must be maximized while deleterious beamstrahlung effects [12] must be minimized. Because the former scales as $1/(\sigma_x\sigma_y)$ [13] (where σ_x and σ_y are the rms beam sizes at the interaction point in the horizontal and vertical plane, respectively) and the latter as $1/(\sigma_x+\sigma_y)$ [14], a common solution is to operate with flat beams, $\sigma_x \gg \sigma_y$ (i.e., with an aspect ratio $\sigma_x/\sigma_y \gg 1$). This motivates the creation of beams with $\epsilon_x/\epsilon_y \gg 1$ (where $\epsilon_{[x,y]}$ is the beam emittance in $[x, y]$) and the preservation of this ratio during acceleration. Established mechanisms that lead to deleterious exchange or mixing of the transverse emittances are linear coupling [15], e.g., due to misaligned or skew quadrupoles, and nonlinear coupling, e.g., due to space-charge effects [16,17], which are mainly relevant at low energies. The latter is linked to the Montague resonance that occurs if the focusing in the horizontal and vertical planes is in phase. Emittance mixing can occur when the motion in the x and y planes is coupled (for instance, when the transverse force in x depends on y), but such effects have not been previously described in plasma-based accelerators.

Plasma accelerators are often operated in the so-called blowout regime, where the driver is strong enough to expel all plasma electrons, creating a trailing ion cavity in its wake. In the ideal case of a uniform background ion distribution within the cavity, the transverse wakefields in x and y are decoupled, preventing emittance exchange. In practice, various nonlinear effects can perturb the transverse wakefields and cause coupling and, hence, emittance mixing. Such effects occur for collider-relevant beams that require high charge (∼nC) and low emittance (∼100 nm) and, therefore, generate extreme space-charge fields capable of ionizing the background plasma to higher levels [18] or causing ion motion [19–21], both of which can lead to the formation of nonlinearly coupled wakefields. Nonlinear wakefields are sometimes desired: For instance, nonlinearities in the wake due to ion motion can suppress the hosing instability [22–24] while still allowing for witness beam emittance preservation through advanced matching schemes [21,25].

In this Letter, we demonstrate by means of theory and 3D particle-in-cell (PIC) simulations that coupled wakefields in plasma accelerators can lead to severe emittance mixing of flat beams when there is a resonance between the betatron oscillations in the horizontal and vertical planes for a large fraction of beam particles. With this effect, the horizontal emittance decreases as the vertical one increases, resulting in an overall growth of their geometric average and, hence, a reduction in luminosity. This mechanism is different from nonlinearity-induced mismatch, by which a beam with a position-momentum distribution not matched to nonlinear fields relaxes at the cost of emittance growth. Unlike emittance mixing, mismatch causes emittance growth in both planes independently. Without proper mitigation, mixing can cause a flat beam to become round, resulting in a considerable decrease in luminosity (e.g., by a factor of 50 for an initial aspect ratio of 100) while

*Contact author: maxence.thevenet@desy.de

simultaneously losing the beneficial suppression of beamstrahlung. This mechanism has direct impact on any future plasma collider design using flat beams. It has previously not been documented, since only short-distance acceleration of flat beams was considered [20].

Emittance mixing for flat beams in coupled, nonlinear wakefields is illustrated with a plasma-wakefield accelerator setup in the blowout regime that resembles the first stage of the proposed hybrid asymmetric linear Higgs factory (HALHF) collider [9]. It consists of an electron drive beam, an electron witness beam, and a singly ionized lithium or argon plasma with a density of $n_0 = 7 \times 10^{15}$ cm^{-3}. Lithium and argon are considered to illustrate the effect of a nonlinearity owing to ion motion and beam-induced ionization, respectively. The drive beam is bi-Gaussian with an rms length of $\sigma_{d,z} = 42$ μm and is located at the origin of the copropagating coordinate system. We chose an emittance of $\epsilon_{d,[x,y],0} = 60$ μm [26]. The witness beam is also bi-Gaussian with initial emittances of $\epsilon_{x,0} = 160$ μm and $\epsilon_{y,0} = 0.54$ μm in the horizontal and vertical planes, respectively. Its length is $\sigma_z = 18$ μm, and it is located on axis, 334 μm behind the drive beam. The drive and witness beams have initial energies of 31.9 GeV ($\gamma_d = 62\,500$) and 5.1 GeV ($\gamma_w = 10\,000$), charges of 4.3 and 1.6 nC, and their transverse rms sizes are matched to the blowout wake. The simulations are conducted with the quasistatic, 3D PIC code HIPACE++ [28] using its mesh refinement capabilities. The complete numerical settings for all the simulations discussed in this Letter are available online [29]. In what follows, $E_0 = m_e c^2 k_p / e$ is the cold, nonrelativistic wave-breaking limit, $k_p = \omega_p / c$ the plasma wave number, $\omega_p = \sqrt{n_0 e^2/(m_e \epsilon_0)}$ the plasma frequency, and ϵ_0 the vacuum permittivity.

Figure 1 shows the nonlinear wake and resulting emittance mixing as the witness beam is accelerated from 5.1 to ∼21 GeV. For a flat witness beam, the large horizontal emittance decreases in lithium by 3.4 μm, or −2%, and in argon by −23%. At the same time, the small vertical emittance increases by 3.4 μm, or +613%, and in argon by +7611%. As collider luminosity scales as the inverse of the geometric average of the transverse emittances $\sqrt{\epsilon_x \epsilon_y}$, this quantity is tracked in the rest of this Letter. In the example in Fig. 1, $\sqrt{\epsilon_x \epsilon_y}$ increases in lithium by +164% (in argon by +670%). Notably, a round beam matched to the same wakefield with the same initial $\sqrt{\epsilon_x \epsilon_y}$ experiences in lithium a small growth of only +0.3% (in argon by +10%) due to mismatch to the nonlinear field. This shows that the drive-beam-induced nonlinearity of the transverse field is the dominant driver of emittance growth in the flat beam case for neither gas.

In the following, we investigate emittance mixing for the regime of nonrelativistic ion motion shown in Fig. 1, by means of test particle simulations. We consider a simplified

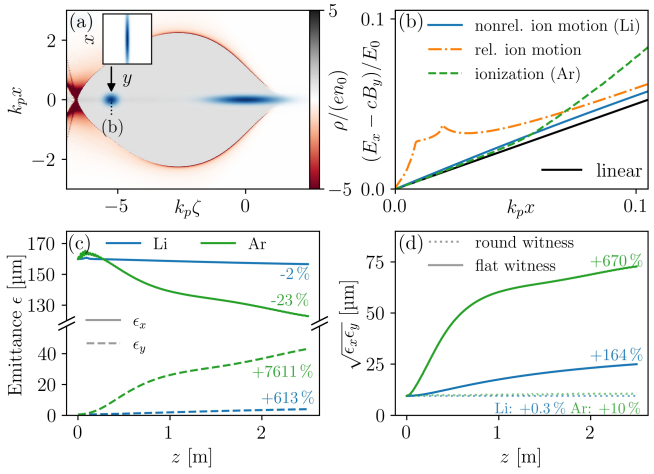

FIG. 1. (a) Normalized plasma charge density (gray-red color scale) and drive and witness beams (blue) in the x-ζ plane, where $\zeta = z - ct$ is the comoving variable and c the speed of light; inset: transverse profile of the flat beam. (b) Examples of nonlinear transverse wakefields. The blue line (nonrelativistic ion motion) corresponds to a lineout along the dashed line of the case in (a). Other colored lines show wakefields with relativistic ion motion (orange), induced by increasing the initial witness beam energy to 478 GeV, thereby decreasing the matched transverse spot size by ∼10×; drive-beam-induced ionization (dashed green line), obtained with argon. (c) Emittance in x (solid lines) and y planes (dashed lines) and (d) $\sqrt{\epsilon_x \epsilon_y}$ for a flat beam in the nonrelativistic ion motion regime (Li, blue lines) and the ionization regime (Ar, green lines) and for corresponding round beams (dotted lines) with the same initial $\sqrt{\epsilon_x \epsilon_y}$.

model based on Ref. [21] that represents well the perturbed transverse wakefield $W_{[x,y]}$ in this regime:

$$W_{[x,y]} = \frac{k_p[x,y]E_0}{2}\left[1 + \alpha_{[x,y]} H\left(\frac{r^2}{2L^2_{[x,y]}}\right)\right], \qquad (1)$$

where $W_x = E_x - cB_y$ and $W_y = E_y + cB_x$ ($E_{[x,y]}$ and $B_{[x,y]}$ are the electric and magnetic fields in the wake, respectively), $H(q) = [1 - \exp(-q)]/q$, $r = (x^2 + y^2)^{1/2}$ is the radius, and $L_{[x,y]}$ and $\alpha_{[x,y]}$ are the characteristic size and amplitude of the nonlinearity, respectively.

Beams of test particles with the same properties as the flat witness beam discussed in Fig. 1 are propagated in the transverse wakefields given by Eq. (1) (assuming no acceleration) for various nonlinearity coefficients $\alpha_{[x,y]}$ and fixed length scales $L_x = L_y = \sigma_{x,d}$. The length scale was chosen to be the drive beam rms size, since the nonrelativistic ion motion is caused by the symmetric drive beam.

The mixing process can be understood by analyzing the single-particle orbits. A beam particle moving in nonlinear wakefields performs transverse betatron oscillations in the x and y planes with frequencies $k_{\beta,x}$ and $k_{\beta,y}$. These frequencies will, in general, differ from the unperturbed

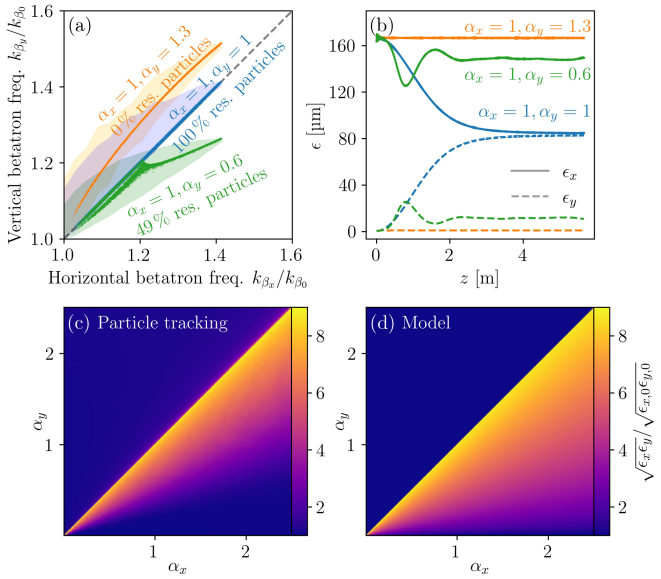

FIG. 2. (a) Distribution of betatron frequencies in the $(k_{\beta,x}, k_{\beta,y})$ plane for three different nonlinearity coefficients $\alpha_y = 1$ (blue points), $\alpha_y = 1.3$ (orange points), and $\alpha_y = 0.6$ (green points). For all cases, $\alpha_x = 1$. The shaded areas denote the initial instantaneous betatron frequencies; the dots show them averaged over many betatron periods. (b) The resulting emittance evolution in x (solid lines) and y (dashed lines). The final $\sqrt{\epsilon_x \epsilon_y}$ at saturation is shown as a function of α_x and α_y for (c) particle tracking and (d) the analytical model from Eq. (2).

betatron frequency $k_{\beta,0} = k_p/(2\gamma_w)^{1/2}$ and depend on the particle's betatron amplitude and, in turn, its initial conditions. Figure 2(a) shows the distribution of betatron frequencies for the beam particles in the three cases considered in Fig. 2(b).

In the presence of a coupling term [assumed weak, $\alpha_{[x,y]} H(r^2/2L^2_{[x,y]}) \lesssim 1$], the x and y orbits form a system of two coupled oscillators. As generally expected from such a system [30], particles satisfying the resonance condition $k_{\beta,x} \simeq k_{\beta,y}$, i.e., near the diagonal in Fig. 2(a), experience an exchange of their horizontal and vertical betatron oscillation amplitudes. This exchange occurs over a timescale much longer than the betatron period. These resonant particles are responsible for the decrease of ϵ_x and increase of ϵ_y. In contrast, for particles far from the resonance, the amplitudes of the oscillations in x and y are both independently preserved. Overall, the fraction of resonant particles in the beam determines the degree of emittance mixing. The case $\alpha_x = \alpha_y = 1$ (blue lines) has 100% resonant particles, which leads to a full equalization of the emittances. For the case $\alpha_x = 1$, $\alpha_y = 1.3$ (orange lines), there are no resonant particles and, hence, no emittance mixing. Finally, in the case of $\alpha_x = 1$, $\alpha_y = 0.6$ (green lines), 49% of the particles are resonant, leading to partial mixing. For more details on the last case, see Supplemental Material [31].

Given the wakefields in Eq. (1), it is possible to estimate the emittances of a flat beam at saturation $\epsilon^*_{[x,y]}$:

$$\epsilon^*_x \simeq \left(1 - \frac{\eta_r}{2}\right)\epsilon_{x,0}, \qquad \epsilon^*_y \simeq (1-\eta_r)\epsilon_{y,0} + \frac{1}{2}\eta_r \frac{\alpha_y}{\alpha_x}\frac{L_x^2}{L_y^2}\epsilon_{x,0}, \tag{2}$$

where

$$\eta_r = \begin{cases} \exp\left[-\frac{4k_p^2 L_x^2 L_y^2}{k_{\beta,0}\epsilon_{x,0}} \frac{\alpha_x - \alpha_y}{3\alpha_x L_y^2 - 2\alpha_y L_x^2}\right], & \alpha_y \le \alpha_x, \\ 0, & \alpha_y > \alpha_x \end{cases} \tag{3}$$

is the fraction of resonant particles in the beam (see Supplemental Material [31] for details).

Figures 2(c) and 2(d) show the relative growth of the geometric emittance, $(\epsilon^*_x \epsilon^*_y/\epsilon_{x,0}\epsilon_{y,0})^{1/2}$, in the (α_x, α_y) plane obtained with particle tracking (c) and with the model (d), respectively. The model reproduces the main qualitative and quantitative observations: Maximal growth of the geometric emittance is observed for $\alpha_x = \alpha_y$ where all beam particles are resonant. When $\alpha_y < \alpha_x$, the fraction of resonant particles decreases, resulting in reduced emittance mixing. For $\alpha_y > \alpha_x$, no resonant particles are present, and, hence, no emittance growth from mixing is observed.

Energy transfer between oscillation modes in coupled oscillators at resonance is a general physics process [30] and can be observed, for instance, in the Wilberforce pendulum [32,33]. The dynamics in a plasma accelerator considered in this Letter are complex, but the emittance exchange process itself does not depend on the specific shape of the nonlinear coupling and is, therefore, observed with any effects causing coupling (e.g., ionization, ion motion, nonuniform plasma density, etc.). Similar to resonance in rf-based accelerators, determining which particles are trapped in the resonance is a nontrivial task, in general [15,34], and requires self-consistent numerical simulations.

Emittance mixing due to resonant particles explains the observed drastic emittance increase in Fig. 1: Since the ion motion (lithium) and ionization (argon) are caused by an axisymmetric drive beam, the resulting coupled, nonlinear fields are axisymmetric. Consequently, all witness beam particles share the same betatron frequency in both the x and y directions, making them resonant and leading to the strong emittance mixing observed.

This observation suggests a possible solution to emittance mixing caused by the drive-beam-induced nonlinear fields: using a flat drive beam to induce asymmetric ion motion and detune the resonance. To confirm this, we ran the simulation from Fig. 1 in lithium with a flat driver. The evolution of the witness beam emittances with both round and flat drive beams is shown in Fig. 3. While the round drive beam with $\epsilon_{d,[x,y],0} = 60$ μm causes large emittance

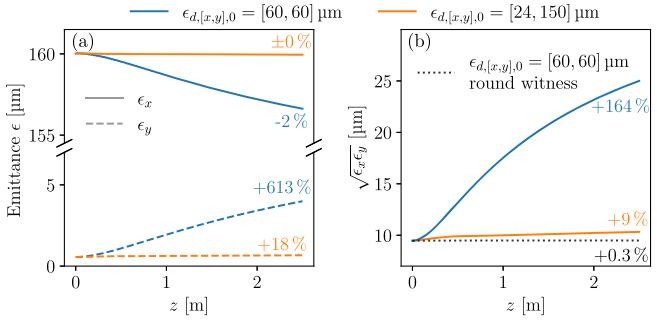

FIG. 3. The evolution of emittances (a) ϵ_x (solid lines) and ϵ_y (dashed lines) and (b) $\sqrt{\epsilon_x \epsilon_y}$, for a flat witness beam and a round driver (blue line), a flat witness beam and a flat driver (orange line), and a round witness and a round driver (gray dotted line).

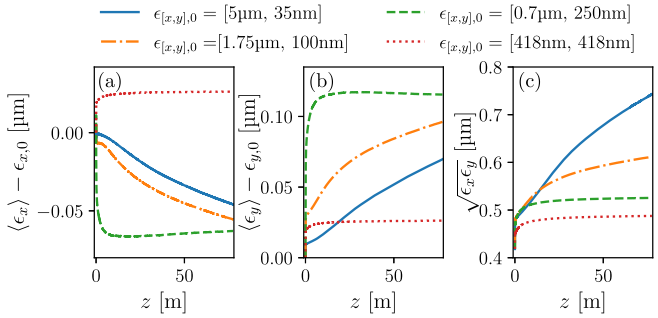

FIG. 4. Evolution of emittances (a) ϵ_x, (b) ϵ_y, and (c) $\sqrt{\epsilon_x \epsilon_y}$, with different initial values for the horizontal and vertical emittances for the witness bunch but the same initial $\sqrt{\epsilon_x \epsilon_y}$. The average slice emittance (subtracted by the initial emittance) is used in (a) and (b) to avoid head-to-tail mismatches that lead to an increase in the emittance in x and mask the mixing, while (c) shows $\sqrt{\epsilon_x \epsilon_y}$.

mixing in the witness beam, a flat drive beam with emittances $\epsilon_{d,[x,y],0} = [24\ \mu\text{m}, 150\ \mu\text{m}]$ causes asymmetric ion motion and suppresses the emittance mixing. The flat driver causes significant ion motion in the y direction and a negligible one in x. The emittance growth in the y direction for the witness beam can be attributed to mismatch in these nonlinear fields rather than emittance mixing, because the emittance does not decrease in the x direction. This growth could, therefore, be prevented by nonlinearly matching the witness beam in y to the nonlinear fields [21,25]. Using a flat drive beam is a viable way to suppress emittance mixing due to drive-beam-induced ion motion, since it breaks the symmetry and, in this case, the resonance.

When the nonlinearity is created by the driver, as above, emittance exchange in the witness beam can be mitigated by shaping the driver. Independently, and regardless of the driver (such that this also applies to laser-driven plasma accelerators), a high-charge, low-emittance, and high-energy witness beam can itself trigger nonlinearities resulting in emittance growth. This is the case, in particular, in the regime relevant for a multi-TeV collider, where the flat witness beam creates nonlinear coupled wakefields due to ion motion or ionization. The induced nonlinearities are not symmetric, because the flat witness beam is not symmetric. Nevertheless, resonance still occurs for enough particles to cause considerable emittance mixing. To assess the emittance mixing in this regime, we choose the same parameters as in Fig. 1 and reduce the witness beam emittance to a level relevant for a future multi-TeV-class collider, namely, $\epsilon_{[x,y],0} = [5\ \mu\text{m}, 35\ \text{nm}]$. At a plasma density of $n_0 = 7 \times 10^{15}\ \text{cm}^{-3}$, the space-charge fields of this matched beam at $\gamma_w = 10\,000$ exceed 300 GV/m, leading to relativistic ion motion. To prohibit ionization effects of the background ions, fully ionized hydrogen is used, although another sufficiently ionized element could be considered. The drive beam is assumed rigid with a large enough emittance not to cause ion motion or ionization to isolate the effects of the witness-beam-induced ion motion. The witness beam is propagated over a distance of 77.5 m and gains energy from 5.1 to 500 GeV.

Figure 4 shows the emittance evolution from four different witness beams with decreasing aspect ratio (from very flat to round with the same initial $\sqrt{\epsilon_x \epsilon_y}$): $\epsilon_{x,0} = 5\ \mu\text{m}, 1.75\ \mu\text{m}, 0.7\ \mu\text{m}$, and 418 nm, while $\epsilon_{y,0} = 35$, 100, 250, and 418 nm, respectively. A modest but fast increase in emittance can be observed at the beginning (in the first 10 cm) due to mismatch in the nonlinear fields, for round and flat beams indiscriminately. After this, the emittance dynamics are governed by mixing. In all flat beam cases, the emittance in x decreases while it increases in y. A flatter beam results in a larger growth of $\sqrt{\epsilon_x \epsilon_y}$, and the emittances of the flattest beams do not reach saturation after acceleration to 500 GeV. The emittances of the flat beams increase by 78%, 46%, and 26%, respectively. The emittance of the round beam increases in both planes by 6% due to the nonlinearity of the ion-motion-perturbed fields, which, again, could be avoided by perfectly matching the beam to the nonlinear fields [21,25].

In this Letter, we have shown that nonlinear transverse wakefields in plasma accelerators couple the particle dynamics in the transverse planes and cause emittance mixing. If not mitigated, this effect can make a flat beam round, resulting in drastic reduction in luminosity. The mixing is due to a resonance between the betatron oscillations in the horizontal and vertical planes, and the most violent emittance mixing occurs for an axisymmetric nonlinear transverse wakefield. This effect can be mitigated by breaking the cylindrical symmetry, which reduces the fraction of resonant particles and, hence, the emittance exchange. For nonlinearities caused by the driver, this can be achieved by tailoring the driver properties with, e.g., flat drive beams or laser drivers (for which ion motion is negligible). Nonlinearities caused by a strong witness beam (high charge, high energy, low emittance), as found in current plasma-based collider designs, also result in considerable beam degradation. This problem needs to be

addressed for future specific designs relying on flat witness beams.

The choice of element used to generate the plasma is decisive: Emittance mixing can be controlled by avoiding both ion motion (stronger for elements with larger charge-to-mass ratio, i.e., light elements or heavy elements ionized to high levels) and beam-induced ionization (stronger for heavy elements when not sufficiently preionized). While only the blowout regime was discussed in detail, emittance mixing can also occur in other regimes such as the linear and quasilinear regimes [35] as well as plasma-based positron acceleration schemes [36–39] that operate with coupled, nonlinear focusing fields. Although hollow core plasma channels [11] could, in principle, be used to avoid emittance mixing, flat beams are then susceptible to beam breakup due to a self-induced quadrupole moment [36].

Acknowledgments—We acknowledge fruitful discussions with Reinhard Brinkmann, Carl A. Lindstrøm, Ming Zeng, Rob Shalloo, and Eric Esarey. We acknowledge the Funding by the Helmholtz Matter and Technologies Accelerator Research and Development Program. This work was supported by the Director, Office of Science, Office of High Energy Physics, of the U.S. Department of Energy, under Contract No. DE-AC02-05CH11231, and used the computational facilities at the National Energy Research Scientific Computing Center (NERSC). We gratefully acknowledge the Gauss Centre for Supercomputing e.V. for funding this project by providing computing time through the John von Neumann Institute for Computing (NIC) on the GCS Supercomputer JUWELS at Jülich Supercomputing Centre (JSC). This research was supported in part through the Maxwell computational resources operated at Deutsches Elektronen-Synchrotron DESY, Hamburg, Germany. This work was funded by the Deutsche Forschungsgemeinschaft (DFG, German Research Foundation)—491245950.

[1] T. Tajima and J. M. Dawson, Phys. Rev. Lett. **43**, 267 (1979).
[2] P. Chen, J. M. Dawson, R. W. Huff, and T. Katsouleas, Phys. Rev. Lett. **54**, 693 (1985).
[3] I. Blumenfeld, C. E. Clayton, F.-J. Decker, M. J. Hogan, C. Huang, R. Ischebeck, R. Iverson, C. Joshi, T. Katsouleas, N. Kirby, W. Lu, K. A. Marsh, W. B. Mori, P. Muggli, E. Oz, R. H. Siemann, D. Walz, and M. Zhou, Nature (London) **445**, 741 (2007).
[4] A. J. Gonsalves, K. Nakamura, J. Daniels, C. Benedetti, C. Pieronek, T. C. H. de Raadt, S. Steinke, J. H. Bin, S. S. Bulanov, J. van Tilborg *et al.*, Phys. Rev. Lett. **122**, 084801 (2019).
[5] C. Aniculaesei *et al.*, Matter Radiat. Extremes **9**, 014001 (2023).
[6] M. Litos *et al.*, Nature (London) **515**, 92 (2014).
[7] M. Kirchen, S. Jalas, P. Messner, P. Winkler, T. Eichner, L. Hübner, T. Hülsenbusch, L. Jeppe, T. Parikh, M. Schnepp, and A. R. Maier, Phys. Rev. Lett. **126**, 174801 (2021).
[8] C. A. Lindstrøm *et al.*, Phys. Rev. Lett. **126**, 014801 (2021).
[9] B. Foster, R. D'Arcy, and C. A. Lindstrøm, New J. Phys. **25**, 093037 (2023).
[10] E. Adli, J.-P. Delahaye, S. J. Gessner, M. J. Hogan, T. Raubenheimer, W. An, C. Joshi, and W. Mori, in *Proceedings, Community Summer Study 2013: Snowmass on the Mississippi (CSS2013): Minneapolis, MN, USA, 2013* (2013), arXiv:1308.1145.
[11] C. Schroeder *et al.*, J. Instrum. **18**, T06001 (2023).
[12] J. E. Augustin, N. Dikansky, Y. Derbenev, J. Rees, B. Richter, A. Skrinsky, M. Tigner, and H. Wiedemann, eConf C **781015**, 009 (1978), https://www.slac.stanford.edu/econf/C781015/pdf/009.pdf.
[13] D. Schulte, Rev. Accel. Sci. Techol. **09**, 209 (2016).
[14] C. Schroeder, C. Benedetti, S. Bulanov, D. Terzani, E. Esarey, and C. Geddes, J. Instrum. **17**, P05011 (2022).
[15] D. A. Edwards and M. J. Syphers, *An Introduction to the Physics of High Energy Accelerators*, Wiley Series in Beam Physics and Accelerator Technology (Wiley, New York, 2008).
[16] B. W. Montague, Fourth-order coupling resonance excited by space charge forces in a synchrotron (1968), https://cds.cern.ch/record/275769/files/CERN-68-38.pdf.
[17] I. Hofmann, *Space Charge Physics for Particle Accelerators* (Springer, New York, 2017).
[18] D. L. Bruhwiler, D. Dimitrov, J. R. Cary, E. Esarey, W. Leemans, and R. E. Giacone, Phys. Plasmas **10**, 2022 (2003).
[19] J. B. Rosenzweig, A. M. Cook, A. Scott, M. C. Thompson, and R. B. Yoder, Phys. Rev. Lett. **95**, 195002 (2005).
[20] W. An, W. Lu, C. Huang, X. Xu, M. J. Hogan, C. Joshi, and W. B. Mori, Phys. Rev. Lett. **118**, 244801 (2017).
[21] C. Benedetti, C. B. Schroeder, E. Esarey, and W. P. Leemans, Phys. Rev. Accel. Beams **20**, 111301 (2017).
[22] T. J. Mehrling, C. Benedetti, C. B. Schroeder, E. Esarey, and W. P. Leemans, Phys. Rev. Lett. **121**, 264802 (2018).
[23] S. Diederichs, C. Benedetti, M. Thévenet, E. Esarey, J. Osterhoff, and C. B. Schroeder, Phys. Rev. Accel. Beams **25**, 091304 (2022).
[24] S. Diederichs, C. Benedetti, E. Esarey, M. Thévenet, J. Osterhoff, and C. B. Schroeder, Phys. Plasmas **29**, 043101 (2022).
[25] C. Benedetti, T. J. Mehrling, C. B. Schroeder, C. G. R. Geddes, and E. Esarey, Phys. Plasmas **28**, 053102 (2021).
[26] The emittance of the drive beam was left as an open parameter in the HALHF proposal but has a strong impact on the design: While a larger emittance increases the deleterious effect of head erosion [27], a small emittance increases driver-induced ion motion or ionization. An emittance of $\epsilon_{d,[x,y]} = 60$ μm was found to be a reasonable trade-off.
[27] W. An, M. Zhou, N. Vafaei-Najafabadi, K. A. Marsh, C. E. Clayton, C. Joshi, W. B. Mori, W. Lu, E. Adli, S. Corde, M. Litos, S. Li, S. Gessner, J. Frederico, M. J. Hogan, D. Walz,

J. England, J. P. Delahaye, and P. Muggli, Phys. Rev. Accel. Beams **16**, 101301 (2013).
[28] S. Diederichs, C. Benedetti, A. Huebl, R. Lehe, A. Myers, A. Sinn, J.-L. Vay, W. Zhang, and M. Thévenet, Comput. Phys. Commun. **278**, 108421 (2022).
[29] S. Diederichs, C. Benedetti, A. Ferran Pousa, A. Sinn, J. Osterhoff, C. B. Schroeder, and M. Thévenet, Input scripts for "Emittance mixing of flat beams in plasma accelerators" (2024), https://zenodo.org/records/10647219.
[30] A. Kovaleva and L. I. Manevitch, Phys. Rev. E **88**, 022904 (2013).
[31] See Supplemental Material at http://link.aps.org/supplemental/10.1103/PhysRevLett.133.265003 for further details on the trapping in the resonance and an analytical model for emittance mixing.
[32] L. R. Wilberforce, London Edinburgh Dublin Phil. Mag. J. Sci. **38**, 386 (1894).
[33] R. E. Berg and T. S. Marshall, Am. J. Phys. **59**, 32 (1991).
[34] G. Guignard, The general theory of all sum and difference resonances in a three-dimensional magnetic field in a synchrotron, technical report No. 1, European Organization for Nuclear Research, 1976, 10.5170/CERN-1976-006.
[35] E. Esarey, C. B. Schroeder, and W. P. Leemans, Rev. Mod. Phys. **81**, 1229 (2009).
[36] S. Zhou, J. Hua, W. An, W. B. Mori, C. Joshi, J. Gao, and W. Lu, Phys. Rev. Lett. **127**, 174801 (2021).
[37] K. V. Lotov, Phys. Plasmas **14**, 023101 (2007).
[38] T. Silva, L. D. Amorim, M. C. Downer, M. J. Hogan, V. Yakimenko, R. Zgadzaj, and J. Vieira, Phys. Rev. Lett. **127**, 104801 (2021).
[39] S. Diederichs, T. J. Mehrling, C. Benedetti, C. B. Schroeder, A. Knetsch, E. Esarey, and J. Osterhoff, Phys. Rev. Accel. Beams **22**, 081301 (2019).